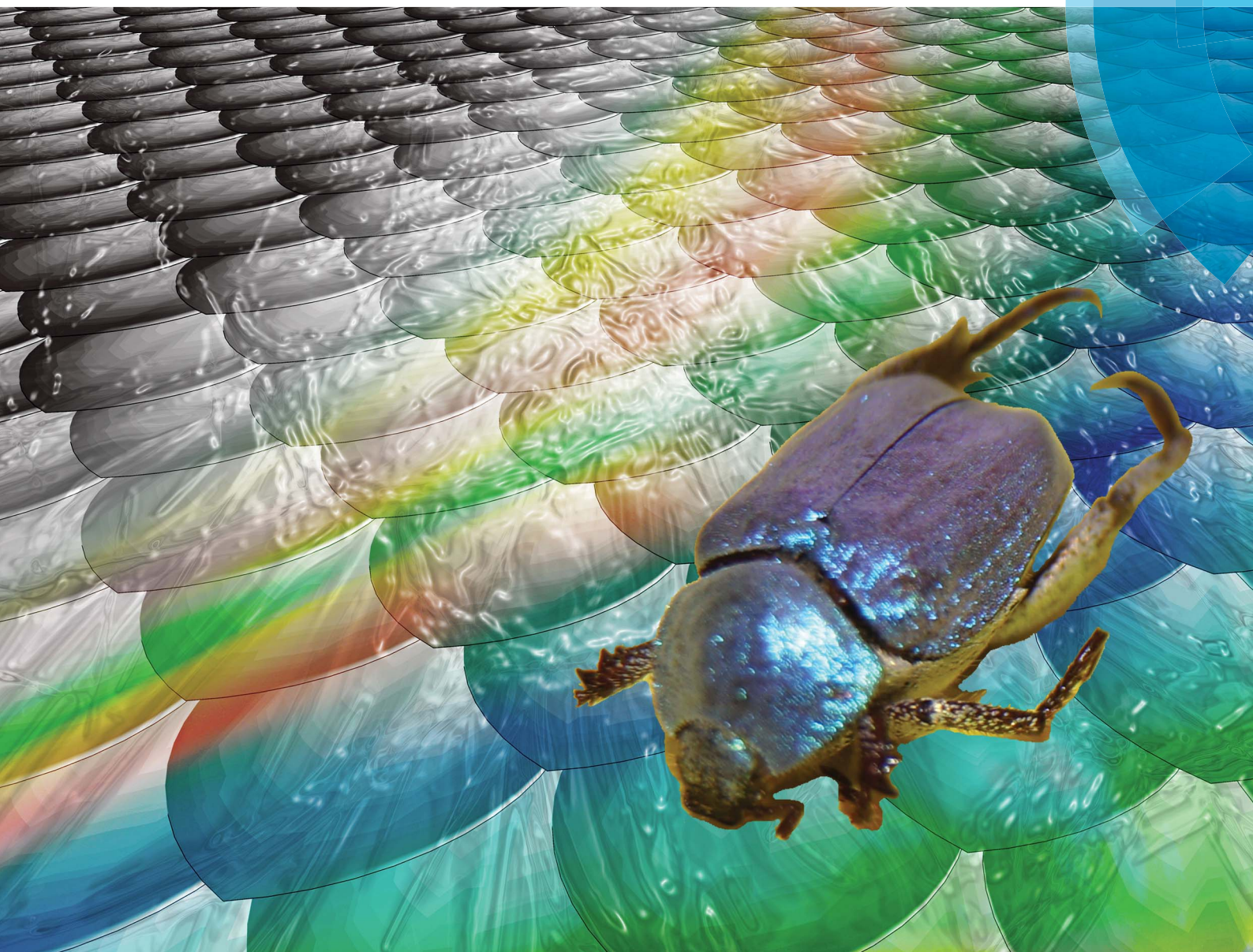


# Journal of Materials Chemistry A

Materials for energy and sustainability

[www.rsc.org/MaterialsA](http://www.rsc.org/MaterialsA)



ISSN 2050-7488



ROYAL SOCIETY  
OF CHEMISTRY

**COMMUNICATION**

Jiayin Yuan *et al.*

Microstructure replication of complex biostructures *via* poly(ionic liquid)-assisted carbonization

CrossMark  
click for updatesCite this: *J. Mater. Chem. A*, 2015, 3, 5778Received 7th January 2015  
Accepted 3rd February 2015

DOI: 10.1039/c5ta00149h

www.rsc.org/MaterialsA

## Microstructure replication of complex biostructures *via* poly(ionic liquid)-assisted carbonization†

Martina Ambrogi, Karoline Täuber, Markus Antonietti and Jiayin Yuan\*

Microstructure transcription of opalescent beetles into functional carbon “bugs” *via* poly(ionic liquid)-assisted carbonization was reported. The presence of a thin coating layer of PIL bearing a dicyanamide anion was found to provide the most precise microstructure preservation even under aerobic combustion conditions.

Natural products are not only renewable, large quantity resources to sustain our society in multiple fashions, but they also possess highly complex hierarchical microarchitectures that inspire and motivate materials scientists to understand their superior structure–property–function relationships. Such knowledge can then be applied in designing bio-inspired and bio-mimetic systems with enhanced characteristics and performances.<sup>1–3</sup> More specifically, carbon materials have attracted tremendous interest recently, especially in the field of energy generation, storage and conversion. Carbon synthesis in cultural history started as a sustainable production from renewable natural raw materials, such as biomass, mostly plant and animal wastes, but this is also highly appreciated in actual science.<sup>4–7</sup> For example, hydrothermal carbonization (HTC) enables the large-scale production of carbonaceous materials under relatively mild conditions in water.<sup>8–10</sup> Besides HTC, physical and/or chemical activation is among the popular methods to convert biomass to porous carbons.<sup>6,10,11</sup> Natural cellulose and chitin are the most abundant polysaccharides in the world, and both already widely used as carbon precursors.<sup>12–14</sup>

Structural preservation of the hierarchical biological morphology *via* carbonization is a convenient approach to lever on the optimized, existing structures with great simplicity, but these approaches are just at their beginning. MacLachlan *et al.* recently reported the synthesis of layer-structured nitrogen-doped carbon material *via* carbonization of nanocrystalline chitin/silica composite. The nematic liquid-crystalline chitin was

first obtained by sequential deacetylation and hydrolysis of the fibrils of king crab shell, which was encapsulated in sol–gel silica and finally carbonized at high temperature.<sup>15</sup> In another example, iron acetate was infiltrated into a leaf and further pyrolyzed at 700 °C. The as-obtained replica, the inorganic “leaf”, kept the microscale leaf skeleton framework but was in addition magnetic and electrochemically active.<sup>16</sup> These examples pointed out, besides the transformation of biomass to functional materials, the possibility to preserve the fine, even artistic structural features of biological systems *via* carbonization, forming a type of “petrified” carbon fossil.

It is the purpose of this paper to show that a new class of charged polymers, poly(ionic liquid)s or polymerized ionic liquids (PILs), can stimulate such a carbonization process and enables preservation even of finest details of the original bio-template. PILs in general are intensively studied currently because of their unusual characteristics, such as high structural density of the ionic liquid (IL) species, surface activity and high thermal and electrochemical stability.<sup>17–20</sup> The presence of heteroatoms in their molecular structure (such as N, S, P and B) and the broad structural tuneability makes PILs a versatile precursor for (graphitic) heteroatom-doped carbons with enhanced conductivity, basicity and oxidation-resistance, and opens up a wide application spectrum in catalytic and electrochemical fields.<sup>21–23</sup> In spite of their high stability, PILs have already been reported to act as an activation agent to convert natural products into porous carbons. For instance, adding a small fraction of PILs throughout an HTC process on biomass could increase the specific surface area and the carbonization yield.<sup>22</sup> Closer to the present work, when PIL was blended with cellulose filter papers or natural cotton, it was possible to obtain shaped, mechanically flexible, fire-retardant, porous nitrogen-doped carbons *via* pyrolysis under nitrogen due to a favourable reaction of the PIL with the sugar units in these biomass sources.<sup>24</sup>

Bearing in mind the “carbon fossil” concept, we herein report how PILs can help replicate even more complex and delicate micro-structures, here exemplified with a chitin-based

Max Planck Institute of Colloids and Interfaces, Department of Colloid Chemistry, D-14476 Potsdam, Germany. E-mail: jiayin.yuan@mpikg.mpg.de; Fax: +49-331-5679502; Tel: +49-331-5679552

† Electronic supplementary information (ESI) available: Experimental details and additional characterization data. See DOI: 10.1039/c5ta00149h





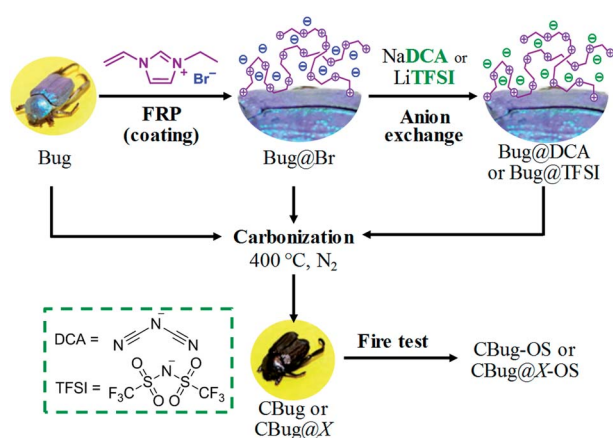
biological species, more specifically a *Hoplia coerulea* beetle (a collected death species). This beetle was chosen as its scales show structural, photonic colour, while its (subtle and delicate) tentacles and legs allow judging the details of replication and the mechanical stability of the product throughout the process very easily. The dead beetle was surface-coated with a PIL layer and subsequently pyrolyzed under nitrogen atmosphere; this process is expected to generate a structure with highly improved thermal and oxidation stability. In a typical run, the beetles were first functionalized with PILs on their surface *via in situ* free radical polymerization of the corresponding IL monomer in dimethylformamide (DMF). After washing with pure solvent to eliminate unanchored polymer chains, they were subsequently converted into carbonaceous beetles at 400 °C under nitrogen. The different counter anions of the PILs play an important role in maintaining the structural information at microscale and were thus systematically investigated. The final combustion test of the carbon beetles directly in air was performed to examine their oxidation resistance. For the sake of conciseness, the uncoated beetles are named “Bug” while the PIL-coated ones are named “Bug@X”, in which X denotes the counter-anion type. Carbonized products are depicted as “CBug@X”. A schematic representation of the entire process is reported in Scheme 1.

*Hoplia coerulea* is a peculiar type of beetle characteristics of the warm regions of France and Spain; it belongs to the Scarabaeidae family and was firstly described by Druri in 1773.<sup>25</sup> Fig. 1A–F show the typical appearance of head, legs and elytra under the scanning electron microscope and optical microscope. The male species presents a brilliant coloration under visible light, varying from violet to blue depending on the incidence angle of the light. This spectacular coloration is due to the presence of lamellar structured scales (or *squamae*, Fig. 1E, F and H) composed of a regular stacking of chitin multilayers, with intra-parallel rods to hold the 3D framework. These scales are spherical disc-like, with a diameter of 50–70 μm and a thickness of around 3.5 μm. Additionally, they are non-compact structure bearing internal voids, as shown in Fig. 1G. The final photonic effect is thus due to the different

refractive index between chitin (roughly 1.56) and air (1.00) and the particular disposition of the layers. Some intensive study has been carried out previously in order to mimic this structural feature for applications in optical fibers and iridescent materials.<sup>26–29</sup>

To grow a thin PIL layer onto inner and outer surfaces of the beetle, 1-ethyl-3-vinylimidazolium bromide as an IL was used as the starting monomer. In a typical procedure, the monomer, thermal initiator, and the biotemplate were mixed in DMF. This solvent was chosen in order to dissolve eventually protective wax sedimentations on the surface of the beetles. The polymerization was performed at 90 °C for 24 h. During the polymerization, the *in situ* generated PIL chains stuck to the surface of all biological microstructures due to the well-known high surface activity of PILs. After polymerization, the templates were washed with DMF several times and dried at 60 °C under vacuum for two days. Instead of the original blue colour, the beetles assumed a brown coloration, depicting the presence of polymer coating on the surface, which changes the overall refractive index (Fig. 2 top, entry B). The final content of polymer on the beetles was calculated by elemental analysis on the bromine content of Bug@Br to be 12 wt%, and its number average molecular weight is estimated to be 55 kDa (Fig. S2†). For comparison, a control experiment was run without IL monomer and radical initiator, which led to the scales appearing still in the natural colour after drying, attributing that the coloration change is due to the PIL coating.

The nature of counter-ion in PILs is well-known to affect the overall hydrophilicity as well as the thermal cross-linking cascades, such as triazine ring from dicyanamide (DCA) ion, or the participation in the evolution of the pore structure, such as



**Scheme 1** Schematic process representation. FRP: free radical polymerization, OS: oxidation stability and X: Br, DCA, TFSI.

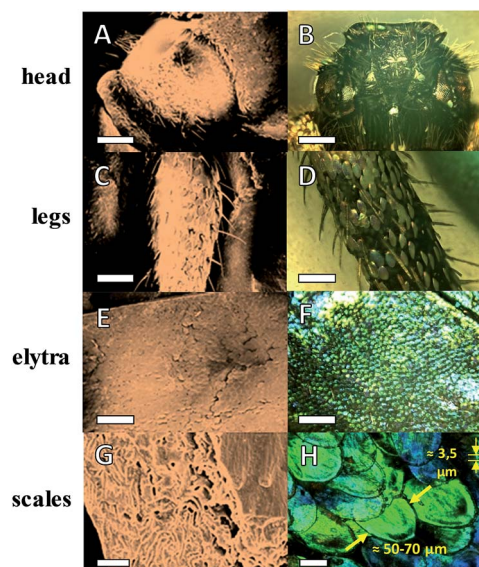


**Fig. 1** SEM (left column) and optical microscope (right column) images of different parts of the beetle *Hoplia coerulea*. From top to bottom are images of head (A and B), legs (C and D), elytra (E and F) and individual scales (G and H). (G) is a cross-section view of a single scale in (H). The numbers in (H) depict the diameter and the thickness of the scale. Scale bars: 500 μm in (A)–(F), 2 μm in (G) & 50 μm in (H).



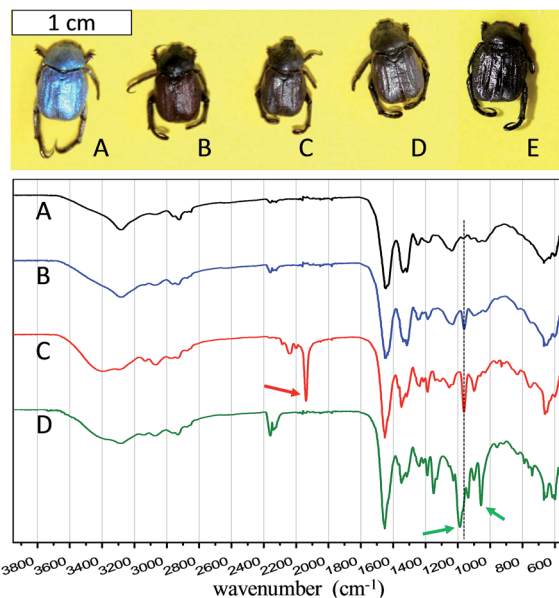


Fig. 2 Photographs (top) and FT-IR spectra (bottom) of beetles and PIL-coated species. (A) Bug, (B) Bug@Br, (C) Bug@DCA, (D) Bug@TFSI and (E) CBug. Note that each beetle represents a different experiment on a different species.

found for bis(trifluoromethanesulfonyl)imide (TFSI).<sup>30</sup> In order to investigate a possible anion effect, anion exchange was performed in DMF to replace Br anion by DCA, and TFSI (Fig. 2 top, entries C and D, respectively).

The successful growth of PIL on the beetle surface was confirmed by Fourier transform infrared spectroscopy (FT-IR, in Fig. 2 bottom). The PIL-coated species with different counter-anions were compared with the pristine species (entry A in Fig. 2). For all the coated beetles, the co-existence of the polymer indicated by the IR peak at  $1162\text{ cm}^{-1}$ , related to the combination of C–C bending and C–N stretching modes of the imidazole ring.<sup>31</sup> Moreover, peaks of the cyano bond at  $2145\text{ cm}^{-1}$ , and of sulfonyl at  $1200\text{ cm}^{-1}$  and of trifluoride at  $1050\text{ cm}^{-1}$  indicate the successful anion exchange from PIL-Br to PIL-DCA (entry C, Fig. 2) and PIL-TFSI (entry D, Fig. 2), respectively. Combustion elemental analysis of all these samples also confirmed the presence of PIL polymer, which led to a slight increase in the nitrogen content from the uncoated Bug (10.8 wt%) to Bug@Br (11.7 wt%, the complete elemental composition is available in Table S1†). It should be noted that the pristine bugs have nitrogen-containing proteins, explaining their nitrogen content. A direct evaluation of the PIL content in the beetle sample was performed by investigating the bromine content in the two samples of Bug and Bug@Br. The absence of Br in case of the pure Bug is obvious, while in the case of Bug@Br a 5 wt% content was observed. Concerning the PIL-DCA and PIL-TFSI coated beetles, the increase in nitrogen content was noticed, which is directly correlated to the nitrogen atoms in the PIL molecular structure (imidazolium and counter anion moieties). In detail, the nitrogen content in Bug@TFSI and Bug@DCA was found to be 11.8 and 12.8 wt% respectively. Scanning electron microscopy (SEM) was applied to visualize

the presence of PILs on the surface of the wings. The results are reported in Fig. 3 (entries A, E, H and K). The presence of the PIL is detectable between the finely structured scales in SEM characterization, creating a rougher and obviously smeared outer surface topology in all PIL/Bug samples.

Thermal gravimetric analysis (TGA) of the uncoated beetle was first performed under both oxygen and nitrogen flow (see Fig. S1†). In the first case complete decomposition was observed at  $650\text{ }^{\circ}\text{C}$ , while heating under nitrogen led to a yield of 20 wt% at  $1000\text{ }^{\circ}\text{C}$ , however losing the main structural features of the template. Carbonization of the original beetle and the PIL-coated beetles were then performed under nitrogen atmosphere at  $400\text{ }^{\circ}\text{C}$ , *i.e.* at the end of the major mass loss in the TGA analysis, in order to investigate the effect of PIL coating on improving the structural stability of the bugs. The final carbon beetles eventually all maintain similar macroscopic appearance, as shown in Fig. 2E. The absence of PIL coating (Fig. 3B, first row) led to obvious destruction of the characteristic lamellar stacking in which the

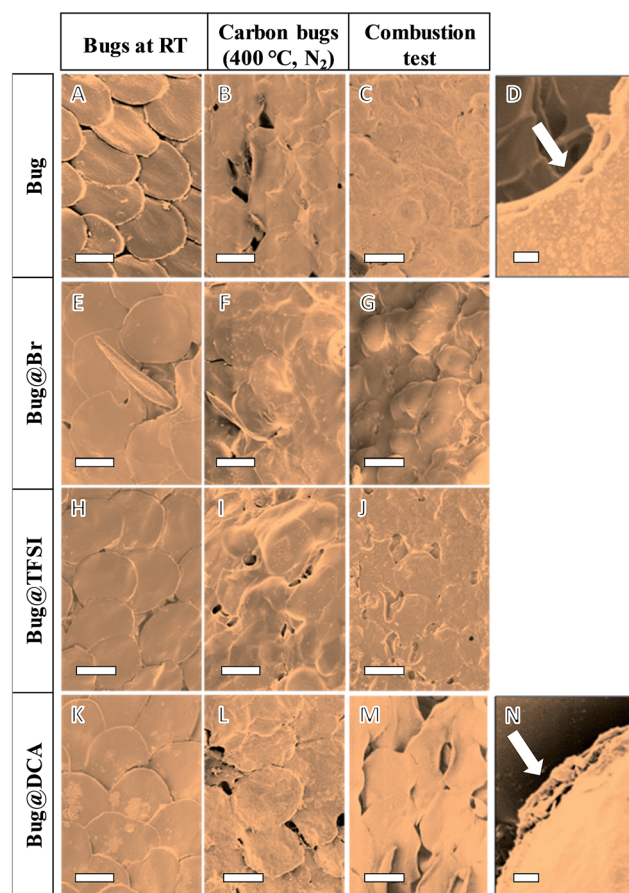


Fig. 3 SEM characterization of intact and PIL-coated bugs (1st column, entries (A) and (B)–(D), respectively), carbonized bugs (2nd column) and results of the burning test on the carbonized bugs (3rd column). In detail: (A) Bug, (B) CBug, (C) CBug-OS (OS: oxidation stability), (E) Bug@Br, (F) CBug@Br, (G) CBug@Br-OS, (H) Bug@TFSI, (I) CBug@TFSI, (J) CBug@TFSI-OS, (K) Bug@DCA, (L) CBug@DCA, (M) CBug@DCA-OS. Scale bar: 50 μm except in (D) and (N) it is 2 μm. (D) and (N) are the cross-section view of single scales in (C) and (M), respectively.





individual scales merge into each other, their structure is melting and collapsing to become hard to be distinguished from each other. Presence of PIL-Br as well as of PIL-TFSI (entries F and I in Fig. 3 respectively) preserves the stack of scales; nevertheless the internal feature of the scales was partially lost. The best result was obtained in the case of CBug@DCA (Fig. 3L), where the contour of individual scales remains visible. This influence of the counter anions on the thermal stability of the scale structure is related to the possibility of these DCA anions to build up cross-linking points at elevated temperature, thus to stabilize the scale morphology. DCA is known to undergo trimerization to form triazine rings to reduce the structural fragmentation.

The carbon beetles were then tested under real combustion conditions, under which the bug samples are otherwise completely destroyed without any protection. Practically in this experiment, the carbon beetles were immersed in ethanol for 15 minutes (the final weight was 2.7 times of the original ones) and then burned in air. The fire temperature close to the carbon template is in the range of 400–600 °C.<sup>32</sup> The final structure of the fired materials was then investigated *via* SEM (entries C, G, J and M in Fig. 3). Again the best results were obtained for CBug@DCA-OS (Fig. 3M), where in fact the specific stacking of the scale pattern remains detectable even after the fire test. A closer view on the internal framework of individual scales showed fine, porous voids, similar to the original micro-architecture (Fig. 3N). Oppositely, the template produced without PIL (CBug-OS, entries C and D in Fig. 3) completely lost both the fine inner morphology as well as the organization pattern of scales. In the case of CBug@Br and CBug@TFSI, only partial structure features of scales were preserved, such as the individual scale outer-ring is detectable in Fig. 3G.

Compared to the scales in the elytra, the other parts of beetles, such as legs and head, are comparably easier to keep structurally during the carbonization, and the function of PILs is less visible. As shown in Fig. 4, the morphology of the hair in the head as well as that on the leg can be replicated at 400 °C in the presence of the PIL-DCA. Such structure details were observed also in the carbon bug without the assistance of PILs.

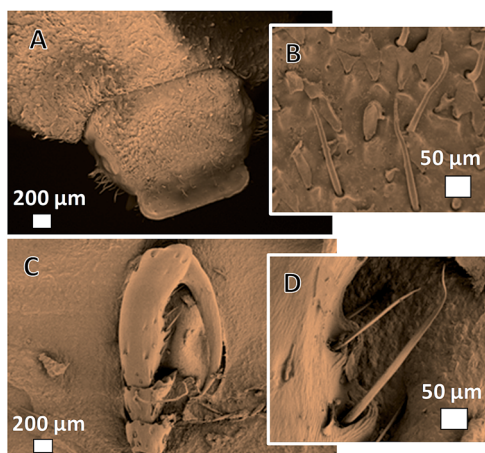


Fig. 4 SEM images of CBug@DCA. (A) head and (C) leg. (B) and (D) are details of the head and the leg, respectively.

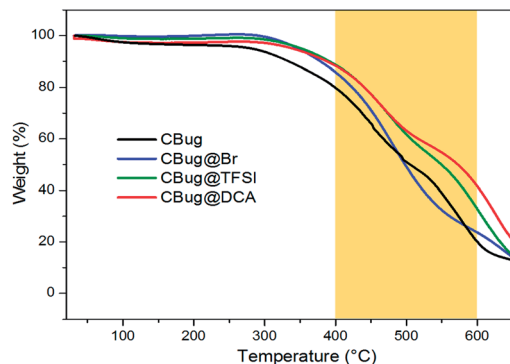


Fig. 5 TGA measurements of different carbon bugs prepared *via* carbonization of beetle samples at 400 °C. The measurements were performed under synthetic air.

To quantify the anti-oxidation effect of PIL to preserve the carbon beetle features, they were examined *via* TGA measurement in air (Fig. 5). The decomposition temperature, here defined as 10 wt% weight lost, is 340 °C for CBug, 380 °C for CBug@Br, and 400 °C for CBug@TFSI and CBug@DCA. Thus, the conversion chemistry induced by the PIL-coating indeed enhanced the thermal stability. At the highest temperature 650 °C, CBug@DCA exhibited still the highest mass residue. Especially in the temperature range from 400 to 600 °C, the mass preservation of CBug@DCA is generally 10–20 wt% larger than that of CBug. This is in good accordance with the above-mentioned combustion test results, in which the CBug@DCA best maintained its structural integrity.

## Conclusions

In summary, we demonstrated the transcription of the micro-structure of an opalescent beetle in functional carbonaceous materials *via* stimulated carbonization with a layer of poly(ionic liquid). It was found that the PIL with the dicyanamide anion gave the most precise microstructure preservation even under aerobic combustion conditions. With this example, we have proven that PILs due to a synergistic effect of their high surface activity, reaction with the carbohydrate template as well as the resulting oxidation stability, have the potential to replicate and preserve even complicated inherent structural motifs of biological templates on the micro- to macroscale.

## Acknowledgements

This work is financially supported by the Max Planck Society and the People Program (Marie Curie Actions) of the European Union's Seventh Framework Program FP7/2007–2013 under REA grant no. 289347. M. Ambrogi would like to thank Dr Laurent Chabanne for the TGA measurements.

## Notes and references

- 1 P. Fratzl and F. G. Barth, *Nature*, 2009, **462**, 442–448.



- 2 R. M. Erb, J. S. Sander, R. Grisch and A. R. Studart, *Nat. Commun.*, 2013, **4**, 1712.
- 3 C. Tamerler and M. Sarikaya, *Acta Biomater.*, 2007, **3**, 289–299.
- 4 D. Saha, Y. Li, Z. Bi, J. Chen, J. K. Keum, D. K. Hensley, H. A. Grappe, H. M. Meyer, S. Dai, M. P. Paranthaman and A. K. Naskar, *Langmuir*, 2014, **30**, 900–910.
- 5 T. Saito, J. H. Perkins, F. Vautard, H. M. Meyer, J. M. Messman, B. Tolnai and A. K. Naskar, *ChemSusChem*, 2014, **7**, 221–228.
- 6 J. Wang, I. Senkovska, S. Kaskel and Q. Liu, *Carbon*, 2014, **75**, 372–380.
- 7 J. Wang, A. Heerwig, M. R. Lohe, M. Oschatz, L. Borchardt and S. Kaskel, *J. Mater. Chem.*, 2012, **22**, 13911–13913.
- 8 A. Jain, S. Jayaraman, R. Balasubramanian and M. P. Srinivasan, *J. Mater. Chem. A*, 2014, **2**, 520–528.
- 9 S.-A. Wohlgemuth, F. Vilela, M.-M. Titirici and M. Antonietti, *Green Chem.*, 2012, **14**, 741–749.
- 10 R. J. White, M. Antonietti and M.-M. Titirici, *J. Mater. Chem.*, 2009, **19**, 8645–8650.
- 11 W. Qian, F. Sun, Y. Xu, L. Qiu, C. Liu, S. Wang and F. Yan, *Energy Environ. Sci.*, 2014, **7**, 379–386.
- 12 A. Dumanlı and A. Windle, *J. Mater. Sci.*, 2012, **47**, 4236–4250.
- 13 L. Heath, L. F. Zhu and W. Thielemans, *ChemSusChem*, 2013, **6**, 537–544.
- 14 M. Nogi, F. Kurosaki, H. Yano and M. Takano, *Carbohydr. Polym.*, 2010, **81**, 919–924.
- 15 T.-D. Nguyen, K. E. Shopsowitz and M. J. MacLachlan, *J. Mater. Chem. A*, 2014, **2**, 5915–5921.
- 16 Z. Schnepp, W. Yang, M. Antonietti and C. Giordano, *Angew. Chem., Int. Ed.*, 2010, **49**, 6564–6566.
- 17 J. Yuan, D. Mecerreyes and M. Antonietti, *Prog. Polym. Sci.*, 2013, **38**, 1009–1036.
- 18 J. Yuan and M. Antonietti, *Polymer*, 2011, **52**, 1469–1482.
- 19 N. Nishimura and H. Ohno, *Polymer*, 2014, **55**, 3289–3297.
- 20 D. Mecerreyes, *Prog. Polym. Sci.*, 2011, **36**, 1629–1648.
- 21 J. S. Lee, X. Wang, H. Luo, G. A. Baker and S. Dai, *J. Am. Chem. Soc.*, 2009, **131**, 4596–4597.
- 22 P. Zhang, J. Yuan, T.-P. Feller, M. Antonietti, H. Li and Y. Wang, *Angew. Chem., Int. Ed.*, 2013, **52**, 6028–6032.
- 23 B. Qiu, C. Pan, W. Qian, Y. Peng, L. Qiu and F. Yan, *J. Mater. Chem. A*, 2013, **1**, 6373–6378.
- 24 Y. Men, M. Siebenburger, X. Qiu, M. Antonietti and J. Yuan, *J. Mater. Chem. A*, 2013, **1**, 11887–11893.
- 25 *Muséum national d'Histoire naturelle, National Inventory of Natural Heritage*, <http://inpn.mnhn.fr>, accessed 2nd December 2014.
- 26 J. P. Vigneron, J.-F. Colomer, N. Vigneron and V. Lousse, *Phys. Rev. E: Stat., Nonlinear, Soft Matter Phys.*, 2005, **72**, 061904.
- 27 E. Van Hooijdonk, S. Berthier and J.-P. Vigneron, *J. Appl. Phys.*, 2012, **112**, 114702–114707.
- 28 D. Olivier, R. Marie, V. Cédric, W. Victoria, V. Jean Pol and L. Stéphane, *New J. Phys.*, 2008, **10**, 013032.
- 29 M. Rassart, P. Simonis, A. Bay, O. Deparis and J. P. Vigneron, *Phys. Rev. E: Stat., Nonlinear, Soft Matter Phys.*, 2009, **80**, 031910.
- 30 J. P. Paraknowitsch, A. Thomas and M. Antonietti, *J. Mater. Chem.*, 2010, **20**, 6746.
- 31 J. L. Lippert, J. A. Robertson, J. R. Havens and J. S. Tan, *Macromolecules*, 1985, **18**, 63–67.
- 32 H. Zhu, T. Kuang, B. Zhu, S. Lei, Z. Liu and S. Ringer, *Nanoscale Res. Lett.*, 2011, **6**, 331.

